The Astronomical Journal, 140:954–961, 2010 October doi:10.1088/0004-6256/140/4/954

PHOTOMETRIC CHARACTERIZATION OF THE GALACTIC STAR CLUSTER TRUMPLER 20

Giovanni Carraro[1,4], Edgardo Costa[2], and Javier A. Ahumada[3]
[1] European Southern Observatory, Alonso de Cordova 3107, Casilla 19001, Santiago 19, Chile; gcarraro@eso.org
[2] Departamento de Astronomía, Universidad de Chile, Casilla 36-D, Santiago, Chile; costa@das.uchile.cl
[3] Observatorio Astronómico, Universidad Nacional de Córdoba, Laprida 854, 5000 Córdoba, Argentina; javier@oac.uncor.edu
Received 2010 May 27; accepted 2010 July 26; published 2010 September 3

ABSTRACT

We present deep *UBVI* photometry for Trumpler 20, a rich, intermediate-age open cluster located at $l = 301.^{\circ}47$, $b = +2.^{\circ}22$ ($\alpha = 12^{h}39^{m}34^{s}$, $\delta = -60^{\circ}37'00''$, J2000.0) in the fourth Galactic quadrant. In spite of its interesting properties, this cluster has received little attention, probably because the line of sight to it crosses the Carina spiral arm twice (and possibly also the Scutum-Crux arm), which causes significant contamination of its color–magnitude diagram (CMD) by field stars, therefore seriously complicating its interpretation. In this paper, we provide more robust estimates of the fundamental parameters of Trumpler 20 and investigate the most prominent features of its CMD: a rich He-burning star clump, and a vertical sequence of stars above the turnoff, which can be either blue stragglers or field stars. Our precise photometry, in combination with previous investigations, has allowed us to derive updated values of the age and heliocentric distance of Trumpler 20, which we estimate to be 1.4 ± 0.2 Gyr and 3.0 ± 0.3 kpc, respectively. As predicted by models, at this age the clump has a tail toward fainter magnitudes and bluer colors, thus providing further confirmation of the evolutionary status of stars in this particular phase. The derived heliocentric distance places the cluster in the inter-arm region between the Carina and Scutum arms, which naturally explains the presence of the vertical sequence of stars (which was originally interpreted as the cluster itself) observed in the upper part of the CMD. Most of these stars would therefore belong to the general galactic field, while only a few of them would be bona fide cluster blue stragglers. Our data suggest that the cluster metallicity is solar and its reddening is $E(B - V) = 0.35 \pm 0.04$. Finally, we believe we have solved a previously reported inconsistency between the spectroscopic temperatures and colors of giant stars in the cluster.

Key words: Galaxy: disk – Galaxy: structure – open clusters and associations: general – open clusters and associations: individual (Trumpler 20)

Online-only material: color figures

1. INTRODUCTION

Observational studies of Galactic open clusters have become a traditional benchmark for testing our comprehension of several aspects of stellar structure and evolution (see Chiosi 2007, and references therein), and also of the formation and properties of the Galactic disk (see Moitinho 2010, and references therein).

Because Galactic open clusters are the clusters immersed in the general Galactic field, it is widely recognized that, unless a detailed star-by-star membership analysis is available (which is *not* the case for the vast majority of Galactic clusters; see Carraro et al. 2008), the interpretation of their color–magnitude diagrams (CMDs) is seriously complicated by field stars located along the line of sight to the cluster. Together with variable extinction, field star contamination can produce sequences in the CMD which resemble typical cluster sequences (especially in the case of very young clusters), leading to erroneous interpretations. Unfortunately, the real nature of these field sequences can only be clarified with a difficult a posteriori membership analysis (Villanova et al. 2004; Moni Bidin et al. 2010).

This work is part of a series of papers aimed at improving the fundamental parameters of poorly studied Galactic clusters (Seleznev et al. 2010; Carraro & Costa 2007, 2009, 2010). Here we address the case of Trumpler 20, whose CMD is obviously dominated by a significant field star population, which has been the cause of past misinterpretations with regard to the cluster itself (Seleznev et al. 2010; Platais et al. 2008, hereafter Pla08; McSwain & Gies 2005).

We present new, deep, *UBVI* photometry that has allowed us to put the fundamental parameters of Trumpler 20 on a firmer base. We study the cluster's CMD in detail and investigate the nature of the conspicuous sequence of bright blue stars in the upper CMD. This latter feature is common in clusters located at low Galactic latitudes, and in this particular case, in the past its presence has led to a misinterpretation of the cluster CMD (McSwain & Gies 2005); here, moreover, we address the question: are these stars blue stragglers (BSs) that belong to the cluster or, more conservatively, are they simply field stars? We also discuss the most prominent feature of the cluster CMD, namely, its clump of He-burning stars, and use it as a distance and age estimator. The clump is possibly the most obvious indication that past classifications and basic parameters of Trumpler 20 (particularly its age) may be in error.

This paper is organized as follows. In Section 2, we summarize previous information available for Trumpler 20. In Section 3, we present our observational material and describe our reduction procedure. The cluster CMD is described in Section 4, while in Sections 5–7 we estimate its basic parameters. Section 8 is devoted to a discussion of the cluster's clump and Section 9 addresses the suspected BS population of Trumpler 20. The global conclusions of the paper, together with suggestions for future research directions, are given in Section 10.

[4] On leave from Dipartimento di Astronomia, Università di Padova, Italy.

2. THE STAR CLUSTER TRUMPLER 20 IN PERSPECTIVE

Trumpler 20 was first noticed by Trumpler (1930), who denoted it as An. 20. He classified the cluster as a III 2r object, namely, a detached cluster with no noticeable concentration, a medium range of brightness between the stars in the cluster, and a rich cluster with over 100 stars. Trumpler estimated a cluster angular diameter of 10 arcmin and a heliocentric distance of 2240 pc. Decades later, Hogg (1965) also identified Trumpler 20 as an 8 arcmin cluster, having 239 probable members down to $V \sim 17$ mag, and van den Bergh & Hagen (1975) described it as a real and rich cluster with an angular diameter of ∼7 arcmin, visible both in the blue and red plates of their homogeneous survey of the southern sky.

More recently, Trumpler 20 was studied by McSwain & Gies (2005), who obtained Strömgren photometry down to $y = 17$ mag in the framework of a search for Be stars in southern open clusters. The sequence they recognized as the main sequence (MS) of Trumpler 20 (see their Figure 59) is, however, most probably composed of field stars because, as recognized by J.-C. Mermilliod (2005, private communication) in the same year, the cluster is much fainter. This prompted an observational campaign which resulted in a much deeper *VI* photometry acquired in 2006, eventually published by Seleznev et al. (2010), which confirmed that Trumpler 20 is actually an old cluster. The same misinterpretation was recognized by Pla08, who secured *BVI* photometry and redetermined the cluster parameters by isochrone fitting, obtaining an age of ∼1.3 Gyr, for $E(B - V) = 0.46$ and $(V - M_V)_0 = 12.15$. This age is consistent with the cluster's CMD, which indeed shows a quite prominent clump, typical of intermediate-age star clusters. The Pla08 parameters are based on a spectroscopic metallicity of [Fe/H] = −0.11, derived from a single red giant star. The authors mention, however, that the value obtained for the reddening raises an inconsistency between the photometric and spectroscopic temperatures. The distance obtained by Pla08 is 3.3 kpc, which puts the cluster much further away than Trumpler's early estimate.

In Seleznev et al. (2010), we combined *VI* optical photometry with Two Micron All Sky Survey (2MASS) data (Skrutskie et al. 2006), and focused our attention mainly on the structure of Trumpler 20. Detailed star count analysis revealed that the cluster has a regular shape and an angular diameter of 10 arcmin, confirming Trumpler's estimate based on a visual inspection. As shown in Figure 7 of Seleznev et al. (2010), the radial density profile is smooth, but the cluster shows a hole in its nominal center. Assuming solar metallicity, we found a reddening consistent with the one derived by Pla08, but a smaller distance of 2.9 kpc, for an age of 1.5 Gyr. Metallicity, together with an insufficient color baseline, may explain these slightly different results.

In an attempt to better characterize this interesting cluster, in 2009 we acquired new deep *UBVI* photometry. The description and interpretation of this photometric material is the subject of this paper. We basically aimed at putting the cluster parameters on a firmer base, and tried to establish whether the blue sequence, erroneously indicated as the MS of Trumpler 20 by McSwain & Gies (2005), is composed of field stars or of cluster BSs.

As can be seen in Figure 1, made from a 900 s *I*-band exposure, Trumpler 20 is barely visible in a very dense stellar field, which complicates the interpretation of its CMD (see below). The field shown in Figure 1 is 20 arcmin on a side: north is at the top and east is to the left.

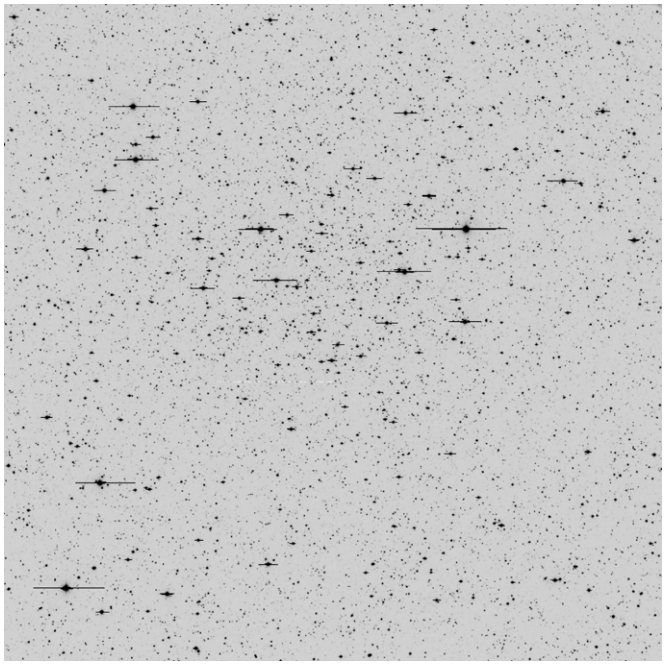

Figure 1. *I*-band 900 s image centered on Trumpler 20. The field is 20 arcmin on a side: north is at the top and east is to the left.

3. OBSERVATIONS AND DATA REDUCTION

3.1. Observations

The region of interest (see Figure 1) was observed with the Y4KCAM camera attached to the Cerro Tololo Inter-American Observatory (CTIO) 1 m telescope, operated by the SMARTS consortium.[5] This camera is equipped with an STA 4064 × 4064 CCD[6] with 15 μm pixels, yielding a scale of 0.″289 pixel^{-1} and a field of view (FOV) of 20′ × 20′ at the Cassegrain focus of the telescope. The CCD was operated without binning, at a nominal gain of 1.44 e^-/ADU, implying a readout noise of 7 e^- per quadrant (this detector is read by means of four different amplifiers).

In Table 1 we present the log of our *UBVI* observations. All observations were carried out in photometric, good-seeing, conditions. Our *UBVI* instrumental photometric system was defined by the use of a standard broadband Kitt Peak $UBVI_{kc}$ set of filters.[7] To determine the transformation from our instrumental system to the standard Johnson–Kron-Cousins system, and to correct for extinction, we observed 46 stars in Landolt's area SA 98 (Landolt 1992) multiple times and with different airmasses ranging from ∼1.1 to ∼2.6. Field SA 98 is very advantageous as it includes a large number of well-observed standard stars, with a very good color coverage: $-0.2 \leqslant (B - V) \leqslant 2.2$ and $-0.1 \leqslant (V - I) \leqslant 6.0$. Furthermore, it is completely covered by the FOV of the Y4KCAM.

3.2. Reductions

Basic calibration of the CCD frames was conducted with the Yale/SMARTS y4k reduction script based on the IRAF[8]

[5] http://www.astro.yale.edu/smarts
[6] http://www.astronomy.ohio-state.edu/Y4KCam/detector.html
[7] http://www.astronomy.ohio-state.edu/Y4KCam/filters.html
[8] IRAF is distributed by the National Optical Astronomy Observatory, which is operated by the Association of Universities for Research in Astronomy, Inc., under cooperative agreement with the National Science Foundation.

Table 1
UBVI Photometric Observations

Target	Date	Filter	Exposure (s)	Airmass
SA 98	2009 Mar 18	*U*	2 × 20, 2 × 150, 2 × 400	1.16–2.08
		B	2 × 20, 2 × 100, 2 × 200	1.16–1.91
		V	2 × 10, 2 × 60, 2 × 120	1.15–1.81
		I	2 × 10, 2 × 60, 2 × 120	1.15–1.72
Trumpler 20	2009 Mar 18	*U*	30, 200, 2000	1.22–1.23
		B	20, 200, 1500	1.28–1.29
		V	10, 100, 900	1.43–1.46
		I	10, 100, 900	1.36–1.38
PG 1047	2009 Mar 18	*U*	2 × 30, 200	1.49–1.52
		B	120	1.47
		V	20, 60	1.40–1.42
		I	2 × 20, 60	1.44–1.45

package CCDRED. For this purpose, zero-exposure frames and twilight sky flats were taken every night. Photometry was then performed using the IRAF DAOPHOT and PHOTCAL packages. Instrumental magnitudes were extracted following the point-spread function (PSF) method (Stetson 1987). A quadratic, spatially variable, master PSF (PENNY function) was adopted. Aperture corrections were determined via aperture photometry of a suitable number (typically 10–20) of bright, isolated, stars in the field. These corrections were found to vary from 0.160 to 0.290 mag, depending on the filter. The PSF photometry was finally aperture corrected, filter by filter.

4. THE PHOTOMETRY

After removing problematic stars and stars having only a few observations in Landolt's (1992) catalog, our photometric solution for a grand total of 297 measurements per filter, turned out to be

$$\begin{aligned} U &= u + (3.080 \pm 0.010) + (0.45 \pm 0.01) \times X \\ &\quad - (0.009 \pm 0.006) \times (U - B), \\ B &= b + (2.103 \pm 0.012) + (0.27 \pm 0.01) \times X \\ &\quad - (0.101 \pm 0.007) \times (B - V), \\ V &= v + (1.760 \pm 0.007) + (0.15 \pm 0.01) \times X \\ &\quad + (0.028 \pm 0.007) \times (B - V), \\ I &= i + (2.751 \pm 0.011) + (0.08 \pm 0.01) \times X \\ &\quad + (0.045 \pm 0.008) \times (V - I). \end{aligned}$$

The final rms of the fitting was 0.030, 0.015, 0.010, and 0.010 in *U*, *B*, *V*, and *I*, respectively.

Global photometric errors were estimated using the scheme developed by Patat & Carraro (2001, their Appendix A1), which takes into account the errors resulting from the PSF fitting procedure (i.e., from ALLSTAR), and the calibration errors (corresponding to the zero point, color terms, and extinction errors). In Figure 2 we present our global photometric errors in *V*, $(B - V)$, $(U - B)$, and $(V - I)$ plotted as a function of the *V* magnitude. Quick inspection shows that stars brighter than $V \approx 20$ mag have errors lower than ∼0.05 mag in magnitude and lower than ∼0.10 mag in $(B - V)$ and $(V - I)$. Higher errors are seen in $(U - B)$.

Our final optical photometric catalog consists of 13,038 entries having *UBVI* measurements down to $V \sim 20$ and 43,471 entries having *VI* measures down to $V \sim 22$.

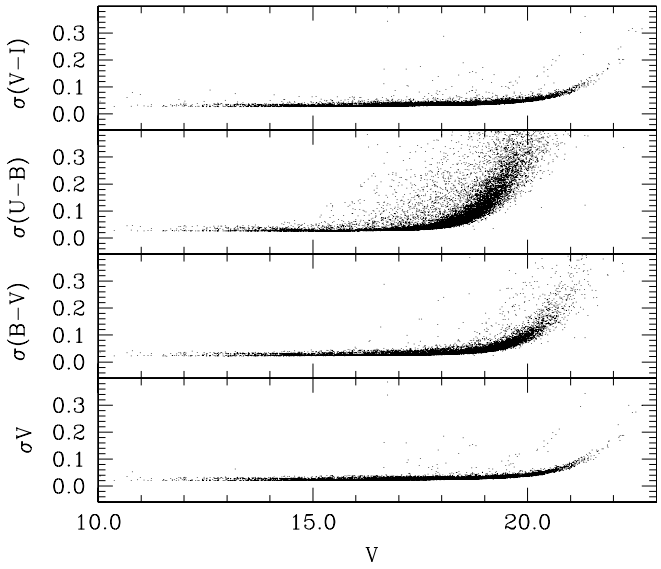

Figure 2. Photometric errors in *V*, $(B - V)$, $(U - B)$, and $(V - I)$ as a function of the *V* magnitude.

4.1. Completeness

Completeness corrections were determined by running artificial star experiments on the data. Basically, we created several artificial images by adding artificial stars to the original frames. These stars were added at random positions and had the same color and luminosity distribution of the true sample. To avoid generating overcrowding, in each experiment we added up to 20% of the original number of stars. Depending on the frame, between 1000 and 5000 stars were added. In this way, we have estimated that the completeness level of our photometry is better than 50% down to $V = 20.5$, and better than 90% down to $V = 19.25$.

4.2. Complementary Infrared Data and Astrometry

Our optical catalog was cross-correlated with 2MASS, which resulted in a final catalog including *UBVI* and JHK_s magnitudes. As a by-product, pixel (i.e., detector) coordinates were converted to R.A. and decl. for J2000.0 equinox, thus providing 2MASS-based astrometry.

Using this $VIJHK_s$ catalog, Seleznev et al. (2010) performed a detailed star count analysis, and derived the radial surface density profile and size of Trumpler 20. In this study, the cluster's center was found to be at $\alpha = 12^{\rm h}39^{\rm m}34^{\rm s}$, $\delta = -60^{\circ}38'42''$, and its diameter and core radius were determined to be ∼30 arcmin and ∼5 arcmin, respectively.

In Section 5.1, we will use these values to estimate field star contamination in the CMDs.

4.3. Comparison with Previous Photometry

In Seleznev et al. (2010) we compared our older *VI* photometry with that of Pla08, and found a good agreement both in *V* and $(V - I)$. Here we present a comparison of our new *BVI* photometry, again with that published by Pla08, in *V*, $(B - V)$, and $(V - I)$. We note that Pla08 do not present *U* photometry. Cross-correlating the two data sets we found 5373 stars in common. The results of this comparison are plotted in Figure 3.

As was found in Seleznev et al. (2010), the comparison is again good in both *V* and $(V - I)$. Given that our photometry is much deeper, the significant scatter seen for *V* fainter than ∼16.0 is clearly due to the increasing errors at the faint tail

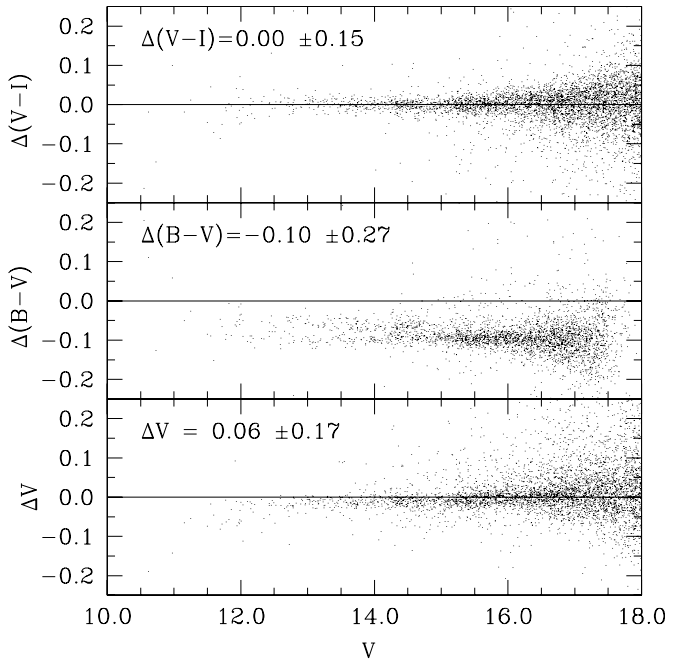

Figure 3. Comparison of our photometry with Pla08 for V, $(B-V)$, and $(V-I)$ as a function of the V magnitude. Comparison is in the sense of our photometry minus Pla08.

of Pla08's photometry. Here we find, however, an important difference in $(B-V)$. In general, this could be due to a variety of reasons, but in this case we believe that the most probable cause is the observing conditions under which the photometry of Pla08 was obtained. These authors admit that they observed few standard stars—with a quite narrow color range—at relatively high airmass. Together with U, the B filter is traditionally the most sensitive to observing conditions and the set of standard stars used. The quite narrow color range can also explain the trend in the V mag comparison, which shows the presence of a shallow unaccounted color term.

As discussed later, this discrepancy could explain the difference we find in $E(B-V)$, and the inconsistency between spectroscopic temperature and color discussed by Pla08.

5. COLOR–MAGNITUDE DIAGRAMS

In Figure 4, we present the CMDs of Trumpler 20, based on all measured stars having photometric errors lower than 0.05 mag, for three different color combinations: V versus $(U-B)$, V versus $(B-V)$, and V versus $(V-I)$.

These CMDs are clearly dominated by dwarf stars (the conspicuous MS) and giant stars from the thin disk (note the sequence departing from the MS at $V \sim 19$–20), located at different distances, and affected by different amounts of extinction. The FIRB reddening in the line of sight (Schlegel et al. 1998) is $E(B-V) = 1.09$, which implies $A_V \sim 3.0$. Given that the line of sight to Trumpler 20 crosses twice the Carina spiral arm, and the Scutum-Crux arm (Russeil 2003), this reddening value (being an integration to infinity) is probably much larger than the one at the distance of the cluster.

A closer inspection of Figure 4 shows the following.

1. The CMD is dominated by a prominent, broad MS extending from the turnoff point at $V \sim 16$ down to the limiting magnitude of our study.
2. At $V \sim 14.5$ there is a conspicuous clump of He-burning stars, which extends significantly in magnitude.
3. A sequence of bright blue stars is seen in the upper left part of the CMDs, extending up to the saturation limit of our data.
4. Many field stars—dwarfs and giants—are spread across the CMD, which complicates the precise definition of all of the above features.

Overall, this CMD closely resembles that of NGC 7789, both in shape and richness. We can say that Trumpler 20 looks like a twin of NGC 7789 (see Section 6).

5.1. Clean Color–Magnitude Diagrams

We have selected cluster members on the basis of their distance from the cluster center. For this, from the star count analysis of Seleznev et al. (2010), we adopted a cluster core radius of 5 arcmin.

Clean CMDs are shown in Figure 5. Field star contamination is still present, but the most important features of the CMDs stand out much better. Most of the stars above the turnoff (TO) have disappeared, which has allowed us to better define its position at $V = 16.0$, $(B-V) = 0.75$, and $(V-I) = 0.85$. While the MS in the V versus $(U-B)$ and V versus $(B-V)$ CMDs is tight and separated from field stars and binaries, the V versus $(V-I)$ MS looks wide, and it appears impossible to separate the cluster's MS from binaries and interlopers. Quite interestingly, the termination point of the MS (the red hook) is still quite blurred, as if several distinct sub-populations were

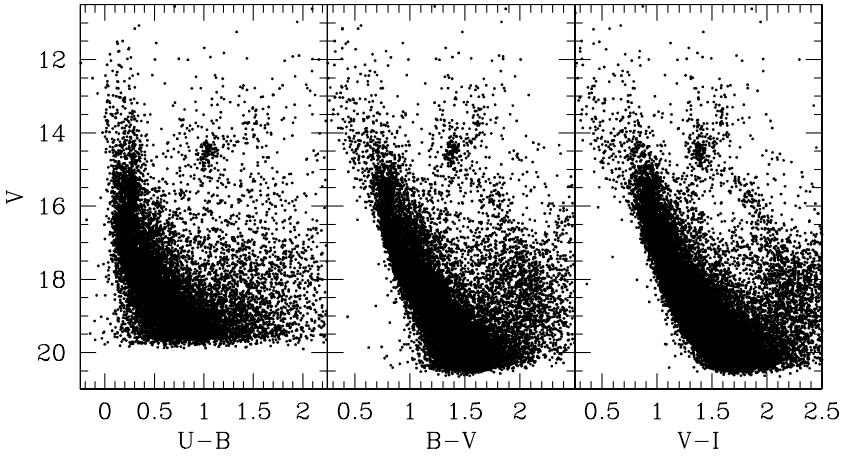

Figure 4. CMDs for three different color combinations based on all measured stars having photometric errors lower than 0.05 mag.

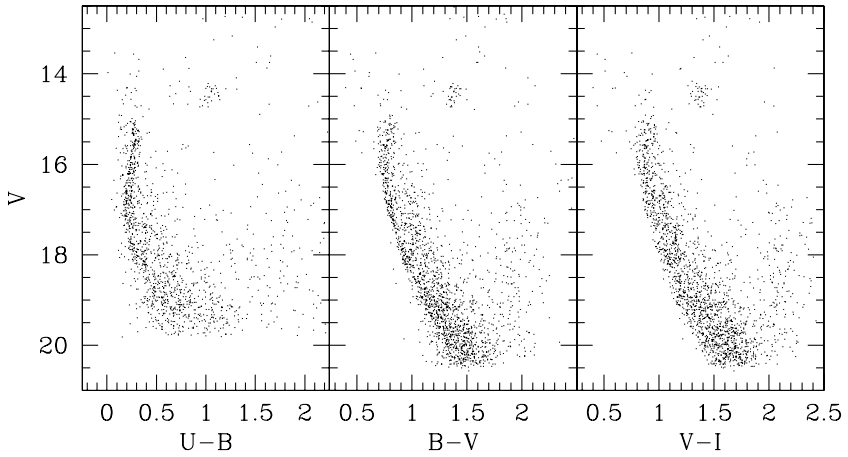

Figure 5. Selection of cluster members on the basis of distance from the cluster center. We have adopted a cluster core radius of 5 arcmin from the star count analysis of Seleznev et al. (2010). The panels are the same as in Figure 4.

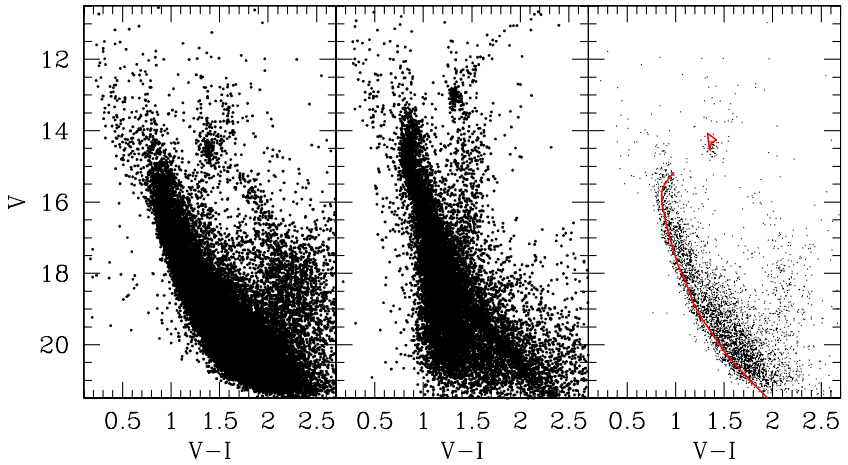

Figure 6. Comparison with NGC 7789. Left panel: Trumpler 20. Middle panel: NGC 7789. Right panel: Trumpler 20 CMD for all stars within the core radius with a superimposed NGC 7789 ridgeline.

(A color version of this figure is available in the online journal.)

present. We believe this is not the case, and will address this point below.

6. EMPIRICAL DETERMINATION OF THE FUNDAMENTAL PARAMETERS: COMPARISON WITH NGC 7789

Anticipating that a comparison of theoretical isochrones with Trumpler 20's CMD is very complicated, due to a very important contamination by disk stars, we have applied an empirical method to derive a first guess of the cluster fundamental parameters.

This exercise is illustrated in Figure 6, where the left panel shows Trumpler 20's CMD, while the middle panel shows that for NGC 7789, from Gim et al. (1998). We will concentrate on these two panels for the moment. Taking into account only their global shape, these two CMDs look similar. They both have thick MSs, sequences of blue stars located along the ideal continuation of the zero age main sequence (ZAMS), and prominent clumps. The MS TO is not clear in any of them. Disk giants are present in both CMDs, although in the case of NGC 7789 they depart from the MS at brighter magnitudes. The differences seen in the precise location of the field stars are the result of their different heliocentric distances and Galactic latitudes, and the different run of interstellar extinction toward them. In fact, NGC 7789 is located 5.°4 below the formal Galactic plane, while Trumpler 20 is at 2.°2 above the plane.

To make this comparison more quantitative and useful, in the rightmost panel of Figure 6 we have considered only stars located inside the core radius of Trumpler 20, and overplotted the ridgeline for NGC 7789. This latter has been shifted by $\Delta V = -0.2$ mag and $\Delta(V - I) = -0.05$ mag. Given that the comparison is quite convincing, we can then assume—as a working hypothesis—that Trumpler 20 has the same metal content as NGC 7789, namely, solar (Gim et al. 1998). Under this assumption, it turns out that the apparent distance modulus of Trumpler 20 is 0.2 mag larger than that of NGC 7789, and that it is slightly more reddened. The reddening of NGC 7789 is $E(V - I) = 0.365$ (Gim et al. 1998), and its apparent distance modulus is $(V - M_V) = 12.2$ mag, which therefore gives $E(V - I) \sim 0.40$ and $(V - M_V) \sim 12.4$ mag for Trumpler 20. These values imply a distance of ∼3 kpc from the Sun for the latter. While the TOs are well matched, the red clump of Trumpler 20 is slightly fainter and redder, which might imply a lower age. We recall that the age of NGC 7789 is around 1.6 Gyr. We shall try to derive the age of Trumpler 20 in Section 8.

7. MORE ON REDDENING AND METALLICITY

Additional insight on the reddening and metallicity of Trumpler 20 can be obtained from the two-color diagram (TCD)

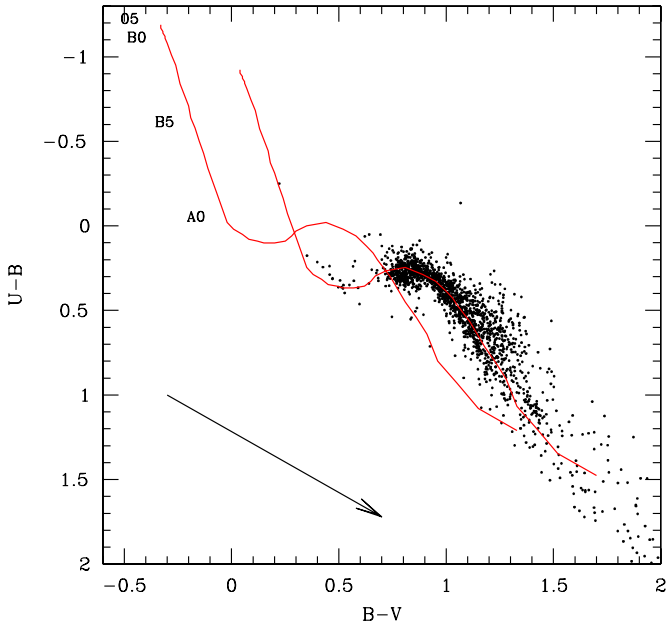

Figure 7. TCD for all stars within 5 arcmin from the center of Trumpler 20, and having photometric errors lower than 0.09 mag in both colors. The solid and dashed lines are empirical ZAMS for zero and 0.35 mag of $E(B-V)$. The normal reddening line is shown in the lower left corner. For illustration purposes, a few spectral types are also indicated.

(A color version of this figure is available in the online journal.)

shown in Figure 7. Again, we consider only stars within the cluster core and with photometric errors lower than 0.09 mag in both colors. The solid line plotted is an empirical ZAMS from Schmidt-Kaler (1982), along which we indicate a few relevant spectral types. The dashed sequence is this same ZAMS, but shifted by $E(B-V) = 0.35$ along the reddening vector (arrow in the bottom left corner of the plot). The fit is reasonable for this value of the reddening, further confirming the results of the previous section.

From the TCD, we can estimate the cluster metallicity by means of the ultraviolet excess index: $\delta_{0.6} = \delta(U-B)(B-V)_0 = 0.6$ (see Sandage 1969; Karatas & Schuster 2006; Carraro et al. 2008). In our TCD, spectral type F stars lie in the range $0.85 \leqslant (B-V) \leqslant 1.0$. We therefore need to look at $(B-V) \approx 0.95$ in this diagram and identify stars whose mean deviation from the ZAMS color is $\delta_{0.6}$. At color $(B-V) = 0.95 \pm 0.05$, we have identified 17 stars that fulfill this condition. Despite the scatter, this value implies [Fe/H] $\sim -0.05 \pm 0.13$, that is, almost solar metal abundance.

8. FITTING THEORETICAL ISOCHRONES TO THE CMD

In Figure 8, we have overplotted solar metallicity theoretical isochrones, from the Padova suite of models (Girardi et al. 2000a), on our V versus $(B-V)$ CMD. Lacking any solid estimate of the metal content of Trumpler 20, we have conservatively adopted a solar metal content (we remind the reader that the value given by Pla08 ([Fe/H] $= -0.11$; Section 2) was obtained from spectroscopy of only one red giant star). We additionally note that the metal content of the *twin* cluster NGC 7789 (Gim et al. 1998) is almost solar.

Adjusting isochrones to a CMD is not an easy and straightforward task, especially in cases like that of Trumpler 20, where contamination from field stars plays an important role. In spite of this, as shown in the left panel of Figure 8, a fit based on the set of parameters discussed previously a reddening of 0.35 mag, a visual apparent distance modulus of 13.7, and an age of 1.4 Gyr matches the cluster MS very well all the way down to our limiting magnitude. We estimate (via by eye inspection) that the uncertainties in $E(B-V)$ and $(V-M_V)$ for this value of the age, are about 0.04 and 0.1, respectively. The reddening-corrected distance modulus is therefore 12.6 mag, which is close to the value derived from the comparison with NGC 7789 within the uncertainties.

The TO is reasonably accounted for, while the isochrone clump has the correct magnitude, but a slightly redder color. We believe this is a problem of the models, which possibly rely

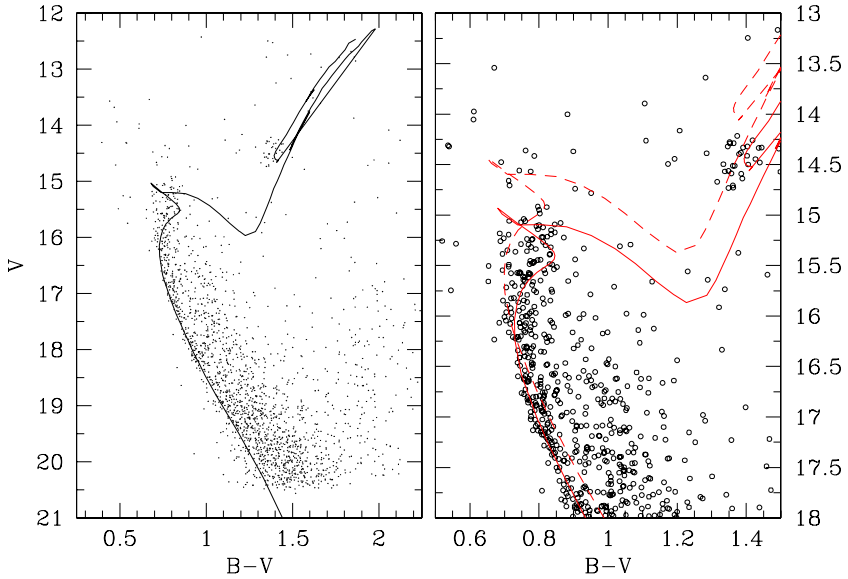

Figure 8. Left panel: isochrone fitting to Trumpler 20 CMD for the set of parameters discussed in Section 7, namely, 0.35 mag, 13.7 mag, and 1.4 Gyr for reddening, distance modulus, and age, respectively. Right panel: a zoom of the TO region. The solid line is the same isochrone as in the left panel, while the dashed one is again the same isochrone but shifted by 0.7 mag to account for unresolved binary stars.

(A color version of this figure is available in the online journal.)

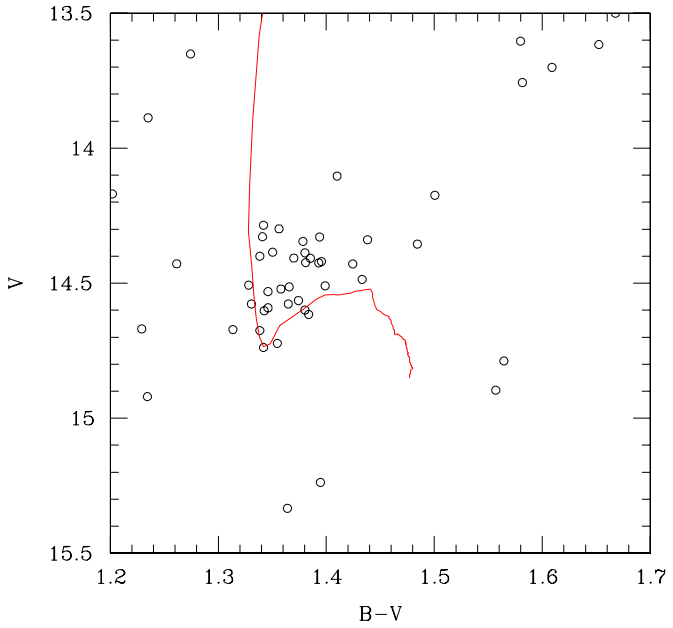

Figure 9. Zoom of the red clump region in the V vs. $(B-V)$ CMD of Trumpler 20. To enhance the features, only stars within the cluster core radius (∼5 arcmin) were plotted. A model from Girardi & Salaris (2001) has been overplotted.

(A color version of this figure is available in the online journal.)

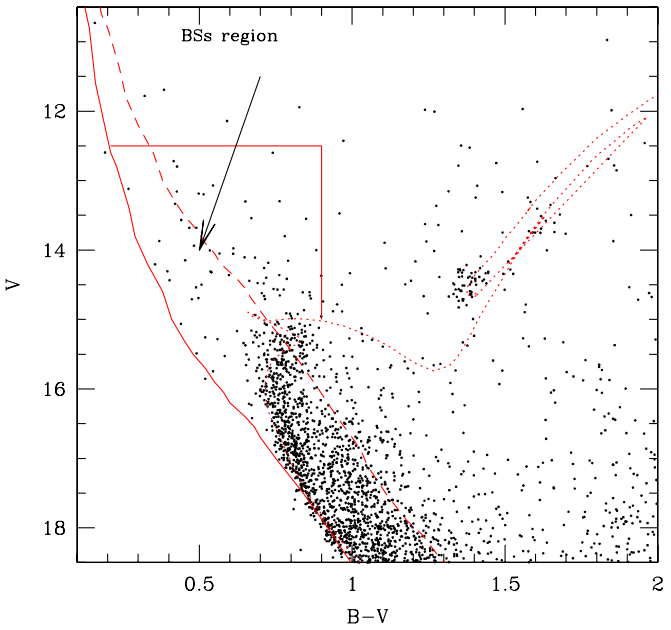

Figure 10. V vs. $(B-V)$ CMD of Trumpler 20 for stars within the core radius. The solid red line is a ZAMS corresponding to the reddening and distance modulus of Trumpler 20, while the red dotted line is an isochrone corresponding to its age, reddening, and distance. The region where BSs are expected to lie is delimited by two straight blue segments, and indicated with an arrow. The green dashed line is a ZAMS displayed for the approximate location and reddening of the Carina spiral arm at the longitude of Trumpler 20.

(A color version of this figure is available in the online journal.)

on poor transformation from the theoretical to the observation plane, and on an imperfect calibration of the mixing length parameter (Carraro & Costa 2007; Palmieri et al. 2002; Moitinho et al. 2006).

To better understand what is happening in the vicinity of the TO, in the right panel of Figure 8 we present a zoom of this region, where the same isochrone is plotted twice; once for the same set of parameters as in the left panel, and a second version shifted by 0.7 mag to account for binary stars. Clearly, the broadening of the MS region is mostly due to unresolved binaries, together with some unavoidable field star contamination (see also the discussion in Section 9).

9. THE RED CLUMP

As shown by Girardi et al. (2000b), the red clump in the Galactic star cluster of this age has a well-defined shape, with an extension to lower magnitudes and bluer color. Given that one of the most interesting features seen in the CMD of Trumpler 20 is its prominent red clump, here we test if the quality of our photometry allows for a study of the detailed morphology of the clump.

To this aim, we need a refined selection of the red clump members. We first tried to perform a preliminary membership analysis using proper motion components from UCAC3 (Zacharias et al. 2010). This effort was not successful, and our conclusion is that this catalog is not useful for studying clusters at large distances from the Sun (3 kpc in the case of Trumpler 20). We therefore used the standard procedure of selecting more probable cluster members on the basis of their distance from the cluster center.

In Figure 9 we show a zoom of the red clump region in the V versus $(B-V)$ CMD of Trumpler 20, considering only stars within 5 arcmin from the cluster center. The red clump of Trumpler 20 indeed shows a structure which closely resembles that of NGC 7789, which we know has a similar age (Girardi et al. 2000b, their Figure 4(a)). In this figure, we have also plotted a model (evolutionary track) from Girardi & Salaris (2001), adopting $E(B-V)=0.35$ and $(V-M_V)=13.7$, as derived above. The fit is reasonable, and provides a further confirmation of the age, reddening, and distance we obtained in previous sections.

As discussed by Girardi et al. (2000b), this morphology of the clump may be resulting either from star-to-star variations in the mass-loss rates during the red giant branch (RGB) phase or by other effects, such as stellar rotation or convective core overshooting, which can cause a significant spread in the core mass at He ignition for stars of similar mass. Apart from NGC 7789 and Trumpler 20, a similar morphology has been found in NGC 2204 and NGC 2660 (Girardi et al. 2000b).

10. THE SEQUENCE OF BRIGHT BLUE STARS: BLUE STRAGGLERS OR FIELD STARS?

The close similarity between the CMDs of Trumpler 20 and NGC 7789 also applies to the population of bright blue stars. These stars can be either field stars located between the cluster and the observer, or BSs (Ahumada & Lapasset 2007). These latter should preferentially lie within the cluster area. According to a recent study by Carraro et al. (2008), in the case of NGC 7789 it turns out that most bright stars in this part of its CMD are interlopers and only a minor percentage are BSs. Here we investigate if the same scenario applies to Trumpler 20.

In Figure 10, we present a V versus $(B-V)$ CMD of Trumpler 20, based only on stars within the cluster's area, and indicate the region where, according to the classic definition (see, e.g., Figure 1 of Ahumada & Lapasset 1995, 2007) BSs should lie. In this diagram, we have overplotted a ZAMS corresponding to its reddening and distance modulus (red solid line), an isochrone corresponding to its age, reddening, and distance (red dotted line), and two straight blue segments indicating the probable

location of BSs (see below for an explanation of the red dashed line). Inside this latter region, we count 65 stars; whether or not these objects are genuine BS members of Trumpler 20 is hard to establish.

Trumpler 20 lies very close to the northern border of the Coalsack dark nebula, in the northern edge of the Carina arm. In this direction, Russeil et al. (1998) found several groups of young stars, three star clusters (NGC 4755, NGC 4463, and NGC 4439), and two H II regions (RCW 69 and RCW 71), all at distances between 1.6 and 2.2 kpc (that is, closer than Trumpler 20), which are consistent with the heliocentric distance and size of the Carina spiral arm. We note that the reddening in these directions to the Carina arm is about 0.35 mag. We may therefore expect that most of the stars close to the green dashed ZAMS in Figure 10 are stars located inside the arm. We note that this ZAMS has been displayed for the mean distance and reddening of the Carina arm (2 kpc and 0.35 mag, respectively), at the longitude of Trumpler 20. Interestingly, this line also crosses the TO region, implying that stars from the Carina arm are significantly blurring the TO region.

We stress that what we are providing here is a mere qualitative description. Only a detailed membership analysis will clarify the real percentage of BSs and field stars.

11. CONCLUSIONS

We have presented deep *UBVI* and wide-field photometry for Trumpler 20, a rich open star cluster, heavily contaminated by field stars, which lies inside the solar ring and in the inter-arm region between Carina and Scutum-Crux. We have exploited our data set aiming to improve our knowledge of the cluster basic parameters. Having repeatedly stressed the crucial role in the interpretation played by high contamination due to field stars, we conclude that Trumpler 20 has an age of 1.4 ± 0.2 Gyr, making it a twin of the better-known open cluster NGC 7789.

As anticipated in the Introduction, Galactic open clusters are ideal laboratories in which to test theories of stellar evolution and to probe Galactic structure. Trumpler 20 appears to be quite a promising confirmation of this.

On the stellar evolution side, we have shown that Trumpler 20 falls in the age range where the clump of He-burning stars exhibits a peculiar morphology, most possibly due to mass-loss variation during the RGB evolutionary phase. Other clusters of this age, such as NGC 2660, NGC 2204, and NGC 7789, are known to have a clump with the same morphology.

On the Galactic structure side, we position Trumpler 20 in the inter-arm region between the Carina and Scutum-Crux arms. We remind the reader that not many clusters of this age are present in the inner disk, possibly because of environmental effects, which prevent the open clusters from surviving for very long (Carraro et al. 2005).

In this respect we believe that a proper spectroscopic study, to better assess membership and metal content, would be really welcome for Trumpler 20. From our photometric study, we can only suggest that its metallicity is probably solar. Knowledge of its metal abundance would be paramount to help constrain the slope and evolution of the radial abundance gradient in the inner disk—where Trumpler 20 lies—which has yet to be explored (Magrini et al. 2009, 2010).

E.C. acknowledges support by the Chilean Centro de Astrofísica (FONDAP No. 15010003) and the Chilean Centro de Excelencia en Astrofísica y Tecnologías Afines (PFB 06). J.A.A. acknowledges ESO for granting a visitorship at ESO premises in Santiago, where part of this work has been done. In the preparation of this paper, we made use of the NASA Astrophysics Data System and the Astro-ph e-print server. This research made use of the WEBDA database operated at the Institute of Astronomy of the University of Vienna, Austria. This work also made extensive use of the SIMBAD database, operated at the CDS, Strasbourg, France. This publication makes use of data products from the Two Micron All Sky Survey, which is a joint project of the University of Massachusetts and the Infrared Processing and Analysis Center/California Institute of Technology, funded by the National Aeronautics and Space Administration and the National Science Foundation.

REFERENCES

Ahumada, J. A., & Lapasset, E. 1995, A&AS, 109, 375
Ahumada, J. A., & Lapasset, E. 2007, A&A, 463, 789
Carraro, G., & Costa, E. 2007, A&A, 464, 573
Carraro, G., & Costa, E. 2009, A&A, 493, 71
Carraro, G., & Costa, E. 2010, MNRAS, 402, 1863
Carraro, G., Méndez, R., & Costa, E. 2005, MNRAS, 356, 647
Carraro, G., Villanova, S., Demarque, P., Moni Bidin, C., & McSwain, M. V. 2008, MNRAS, 386, 1625
Chiosi, C. 2007, in IAU Symp. 239, Convection in Astrophysics, ed. F. Kupka, I. Roxburgh, & K. Chan (Cambridge: Cambridge Univ. Press), 235
Gim, M., Vandenberg, D. A., Stetson, P. B., Hesser, J. E., & Zurek, D. R. 1998, PASP, 110, 1318
Girardi, L., Bressan, A., Bertelli, G., & Chiosi, C. 2000a, A&A, 141, 371
Girardi, L., Mermilliod, J.-C., & Carraro, G. 2000b, A&A, 354, 892
Girardi, L., & Salaris, M. 2001, MNRAS, 323, 109
Hogg, A. R. 1965, Mem. Mount Stromlo Obs., 17, 1
Karatas, Y., & Schuster, W. J. 2006, MNRAS, 371, 1793
Landolt, A. U. 1992, AJ, 104, 372
Magrini, L., Sestito, P., Randich, S., & Galli, D. 2009, A&A, 494, 95
Magrini, L., et al. 2010, A&A, submitted
McSwain, M. V., & Gies, D. R. 2005, ApJS, 161, 118
Moitinho, A. 2010, in IAU Symp. 266, Star Clusters: Basic Galactic Building Blocks Throughout Time and Space, ed. R. de Grijs & J. Lepine (Cambridge: Cambridge Univ. Press), 106
Moitinho, A., Carraro, G., Baume, G., & Vázquez, R. A. 2006, A&A, 445, 493
Moni Bidin, C., de la Fuente Marcos, R., de la Fuente Marcos, C., & Carraro, G. 2010, A&A, 510, 44
Palmieri, R., Piotto, G., Saviane, I., Girardi, L., & Castellani, V. 2002, A&A, 392, 115
Patat, F., & Carraro, G. 2001, MNRAS, 325, 1591
Platais, I., Melo, C., Fullbright, J. P., Kozhurina-Platais, V., Figuera, P., Barnes, S. A., & Mendez, R. A. 2008, MNRAS, 391, 1482 (Pla08)
Russeil, D. 2003, A&A, 397, 133
Russeil, D., Georgelin, Y. M., Amram, P., Gach, J. L., Georgelin, Y. P., & Marcelin, M. 1998, A&AS, 130, 119
Sandage, A. R. 1969, ApJ, 158, 1115
Schlegel, D. J., Finkbeiner, D. P., & Davis, M. 1998, ApJ, 500, 525
Schmidt-Kaler, Th. 1982, in Landolt-Börnstein, Numerical Data and Functional Relationships in Science and Technology, New Series, Group VI, Vol. 2(b), ed. K. Schaifers & H. H. Voigt (Berlin: Springer), 14
Seleznev, A. F., Carraro, G., Costa, E., & Loktin, A. V. 2010, New Astron., 15, 61
Skrutskie, M. F., et al. 2006, AJ, 131, 1163
Stetson, P. B. 1987, PASP, 99, 191
Trumpler, R. J. 1930, Lick Obs. Bull., 14, 154
van den Bergh, S., & Hagen, G. L. 1975, AJ, 80, 11
Villanova, S., Carraro, G., de la Fuente Marcos, R., & Stagni, R. 2004, A&A, 428, 67
Zacharias, N., et al. 2010, AJ, 139, 2184